

# The Continuous Wavelet Transform, a Valuable Analysis Tool to Detect Atmospheric and Ionospheric Signatures in GPS Radio Occultation Phase Delay Data

Achim Helm, Georg Beyerle, Stefan Heise, Torsten Schmidt, and Jens Wickert

GeoForschungsZentrum Potsdam, Dept. 1 'Geodesy & Remote Sensing',  
Telegrafenberg, D-14473 Potsdam, Germany, [helm@gfz-potsdam.de](mailto:helm@gfz-potsdam.de)

**Summary.** GPS radio occultation phase delay (PD) data contain valuable information about atmosphere and ionosphere and its structure, based on the recorded changes of the direct GPS signal between LEO and GPS satellite. PD data contain signatures of surface reflections mainly above water and snow/ice covered regions which have successfully been detected and analyzed with the radio holographic (RH) method recently. Reflection signatures in the PD data can also be detected and analyzed with the continuous wavelet transform (CWT) in a straight forward manner, e.g. without requiring any additional information/forward model or reference field. The use of the CWT as an additional tool to analyze PD data is described and the assets and drawbacks in comparison to RH are discussed. Two years of consistent CHAMP PD data have been analyzed with CWT. The signature of surface reflections can be detected successfully. The CWT based method also reveals weak signatures during times when the direct GPS signal is not influenced by the atmosphere and travels only through the ionosphere. Different classes of ionospheric signatures can be isolated. The geographical distribution of each signature class reveals different patterns. Such observations may contribute to investigations of ionospheric structures like sporadic E or spread F layer.

**Key words:** CHAMP, GPS, Radio occultation, Continuous wavelet transform, CWT, Atmosphere, Ionosphere, Reflections

## 1 Introduction

GPS radio occultation PD data contain valuable information about the atmosphere (e.g., [2]) and ionosphere (e.g., [3], [4]) and its structure, based on the recorded changes of the direct GPS signal between LEO and GPS satellite. [1] already applied a wavelet based method on a simulated occultation signal. This study evaluates qualitatively which signatures beside the direct occultation signal can be retrieved from about 2 years of CHAMP PD data using the CWT [5].

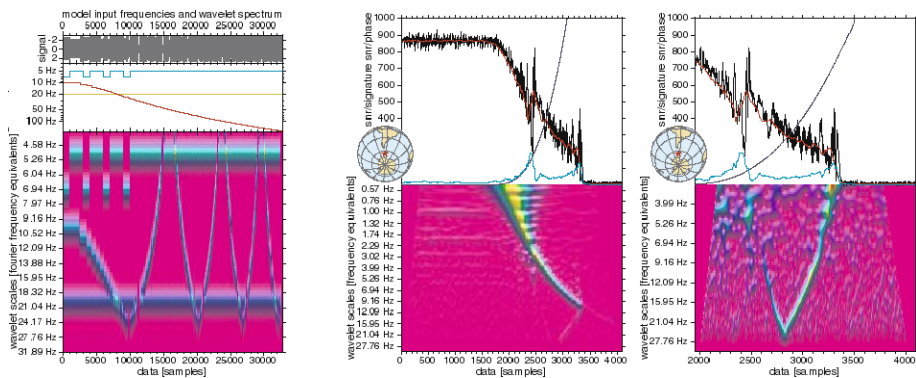


**Fig. 1.** The wavelet spectrum presents low energy by pink, higher energy by blue/green/yellow. The x-axis represents time given in data-samples. The y-axis starts at high frequencies and goes up to lower frequencies. Left: Wavelet spectrum of a model signal composed of different varying frequencies. Middle and right: The amplitude/snr of the PD data is plotted in black, the phase in blue. A running mean of the amplitude is printed in red, its standard deviation in turquoise. A star on the globe marks the location of the occultation. Middle: Wavelet spectrum of CHAMP PD data. Right: Type ATMO-A signature, after subtracting the direct signal.

## 2 Method

The CWT of a discrete sequence is defined as the convolution of the sequence with a scaled and translated version of a function, called the mother wavelet. By varying the wavelet scale and translating along the localized time index, one can construct a two-dimensional picture showing both the amplitude of any features versus the scale and how this amplitude varies with time. The result represents the wavelet energy spectrum. The wavelet function must have zero mean and must be localized in time and frequency. In this study the Morlet wavelet is used. It is constructed of a plane wave and modulated by a Gaussian. The time series must have equal time spacing. The relationship between wavelet scale and Fourier frequency depends on the used wavelet function and can be derived analytically for a particular wavelet function. In the wavelet spectrum signals with constant frequency appear as horizontal lines or as line segments when the signal occurs only sporadically. Frequencies higher than the Nyquist frequency (in this study 25 Hz) are aliased back into the spectrum (Fig. 1, left panel).

CHAMP calibrated atmospheric phase delay data (CH-AI-2-PD) [6] are interpreted as complex time series with a sampling rate of 50 Hz. The signal-to-noise ratio for the L1 Coarse/Aquisition data is used as amplitude and the associated atmospheric phase delay is used as phase. A running mean phase is calculated and subtracted in order to restrain the energy of the direct occultation signal (Fig. 1, middle and left panel). The wavelet energy

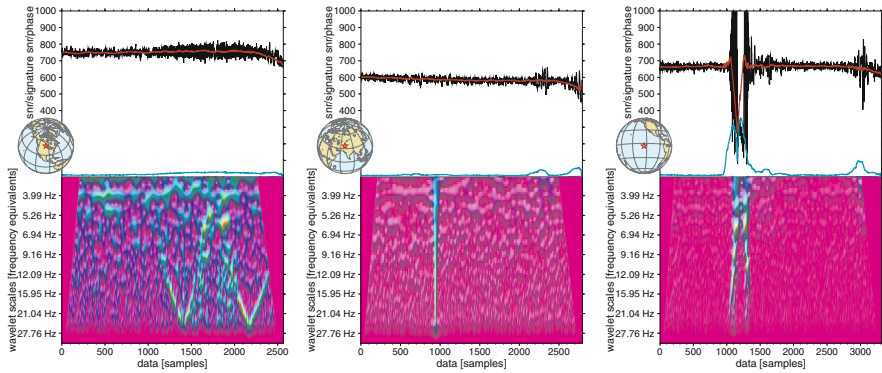


**Fig. 2.** Three different types of ionospheric signatures can be identified with CWT-CS. From left to right: type IONO-A, IONO-B and IONO-C

spectrum is calculated in a 2-dimensional grid and represents the normalized energy at each wavelet scale and discrete time sample. In order to screen the large PD data set a classification scheme (CWT-CS) was developed which automatically analyzes the 2-D wavelet spectrum for structured energy patterns. CWT-CS classifies the energy patterns into 4 characteristic types of signatures which could be regularly observed in the PD data. The signature is classified as atmospheric type ATMO-A (Fig. 1, right panel) in case the energy pattern is observed when the phase delay starts to be influenced by the neutral atmosphere, else as ionospheric type IONO-A, -B or -C (Fig. 2).

### 3 Data Analysis and Discussion

106,160 CHAMP GPS radio occultation events are used from the time period between 14 May 2001 and 22 August 2003. CWT-CS detected 26,870 atmospheric signatures and 14,010 ionospheric signatures which could be separated into 3 different classes, 6,140 of type IONO-A, 2,887 of type IONO-B and 4,983 of type IONO-C. Each signature class reveals a different global distribution pattern (Fig. 3). Most ATMO-A events occur over Antarctica's inland ice and over the shelf ice between  $330^{\circ}$ – $150^{\circ}$ E and  $160^{\circ}$ – $270^{\circ}$ E longitude respectively. Events also cluster at the area of the Bering Sea and the equatorial current belt systems. During a shorter data period (26 August 2001 – 1 February 2002) the CWT-CS detected atmospheric signatures are compared to the results obtained with RH. RH uses a reference model which only allows those rays which undergo a reflection at Earth's surface [2]. From 27,546 recorded CHAMP occultation events RH identifies 6,471 reflection signatures while CWT-CS detects 4,934 ATMO-A signatures. As can be seen in Fig. 3 and [2], CWT-CS can detect strong reflections from ice- and snow covered areas, but unlike RH CWT-CS also registers a large number of

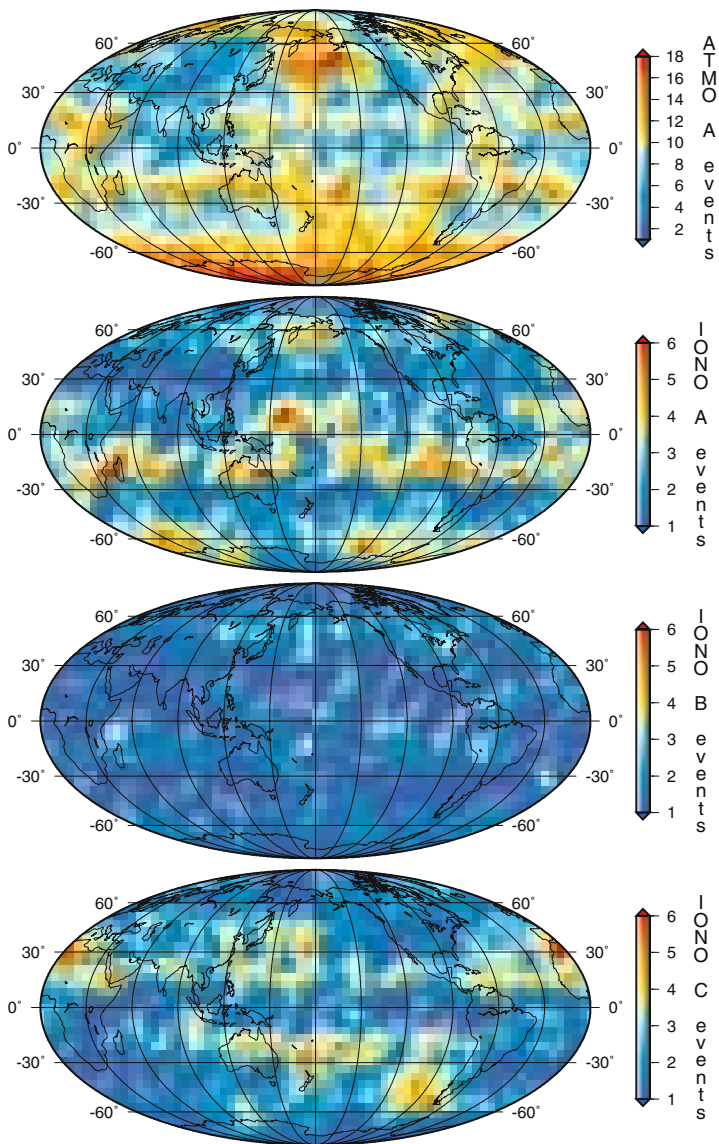


**Fig. 3.** Global distribution of CWT-CS detected signature events using CHAMP PD data between 14 May 2001 and 22 August 2003. A Mollweide projection with a geographical grid of 30° x 30° is used, with the central meridian located at the left border. The events are counted within a global grid of 3° x 3° resolution.

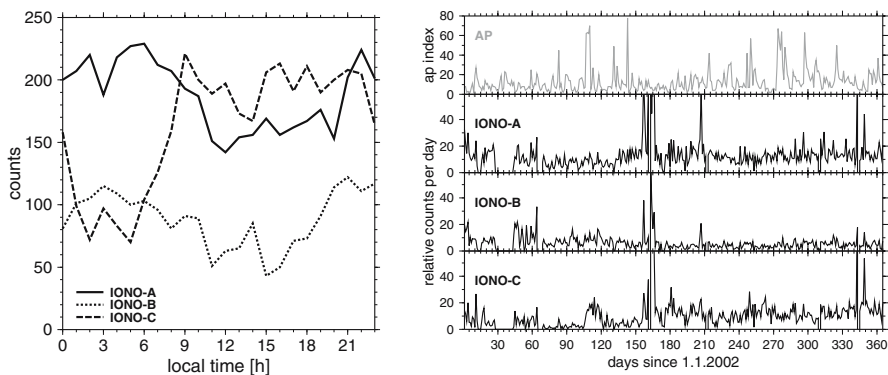


**Fig. 4.** Left: Ionospheric class distribution relative to local time (LT) between 14 May 2001 and 22 August 2003, data excluded from polar regions (above  $\pm 65^\circ$  latitude). Right: Daily occurrence of each ionospheric signature in relation to the daily number of registered PD-data in comparison to the planetary equivalent daily amplitude (Ap) index during 2002.

events at locations on continents where reflections are not expected. IONO-A events can be frequently observed within  $\pm 30^\circ$  latitude with a strong local pattern. Additionally IONO-A events concentrate at the Bering Sea and locations around  $-60^\circ$  latitude. IONO-B events do not show such pronounced local pattern. IONO-C events are mainly distributed between  $\pm 15^\circ$ – $60^\circ$  latitude, in the southern hemisphere roughly limited to the region of the southern pacific ocean. The number of IONO-A and IONO-B events decreases during local-day-time (10:00–20:00 LT), while IONO-C events rapidly drop after local-midnight (01:00–06:00 LT, Fig. 4, left). During 2002 some signals/peaks can be observed in the relative number of all ionospheric signatures (Fig. 4, right), e.g. between day of the year (DOY) 40–65, 155–175 and 340–365. The comparison with magnetic field disturbances represented by the Ap index shows no direct correlation. The highest variability is observed in the IONO-C data set. Between DOY 70–105 only a low number of IONO-C events can be counted daily. From DOY 105–125 a strong increase can be observed while the Ap index has a high amplitude for several days. A similar longer lasting high amplitude of the Ap index (DOY 270–285) does not result in a higher occurrence of IONO-C events.

Taking into account the PD signal form and the height (point of closest approach) of about 90–130 km, IONO-C events can be partly connected to sporadic E. Due to the integral character of PD data, parts of IONO-C events may also be connected to spread F and the equatorial fountain effect because of the geographical pattern and the local time distribution of IONO-C signatures. During IONO-A events longer-lasting amplitude fluctuations can be observed in the PD data. In the CWT spectrum an energy signature can be

observed with a varying frequency shift to the direct PD signal, similar to ATMO-A.

## 4 Conclusions and Outlook

In comparison to CWT-CS RH can better identify surface reflection events. CWT-CS detects 4 different types of signatures in 2 years of CHAMP PD data. All show different geographical distribution patterns. Parts of ATMO-A signatures can be identified as surface reflections and the energy signature can be interpreted as frequency shift of the reflected signal. Parts of IONO-C signatures can be connected to ionospheric structures and may contribute to further investigations of sporadic E or spread F. Additionally, CWT-CS can potentially be used to watch for short and weak noise signals (e.g. 1 Hz in Fig. 1, middle panel, sample 500–1500) in the PD data. Nevertheless CWT-CS offers an adequate tool for analyzing PD data in case no suitable reference model is available or no background information is known, but interpretation of the results is more difficult.

*Acknowledgement.* The authors are very grateful to all the colleagues of the CHAMP team for the given support and data. The National Geophysical Data Center kindly provided the Ap index data.

## References

1. Benzon H and Lauritsen K (2002) Radioholographic and wavelet analyses of radio occultation data. *Geophys Res Abstr*: pp. A–05682.
2. Beyerle G, Hocke K, Wickert J, Schmidt T, and Reigber Ch (2002) GPS radio occultations with CHAMP: A radio holographic analysis of GPS signal propagation in the troposphere and surface reflections. *J Geophys Res* *07(D24)*: doi:10.1029/2001JD001402.
3. Hocke K, Igarashi K, Nakamura M, Wilkinson P, Wu J, Pavelyev A, and Wickert J (2001) Global sounding of sporadic E layers by the GPS/MET radio occultation experiment. *J Atmos Solar-Terr Phys* *63(18)*: 1973–1980.
4. Pavelyev A, Wickert J, Liou Y, Igarashi K, Hocke K, and Huang C (2003) Vertical gradients of refractivity in the mesosphere and atmosphere retrieved from GPS/MET and CHAMP radio occultation data. In: Reigber Ch, Lühr H, and Schwintzer P, eds, *First CHAMP Mission results for Gravity, Magnetic and Atmospheric Studies*, Springer: 500–507.
5. Torrence Ch and Compo GP (1998) A practical guide to wavelet analysis. *Bull Amer Meteor Soc* *79*: 61–78.
6. Wickert J, Galas R, Beyerle G, König R, and Reigber Ch (2001) GPS ground station data for CHAMP radio occultation measurements. *Phys Chem Earth (A)* *26(6-8)*: 503–511.